

Ultralight Helicopter with Trailing-Edge Flap for Primary Control

Jinwei Shen *

Inderjit Chopra †

Alfred Gessow Rotorcraft Center
Department of Aerospace Engineering
University of Maryland, College Park, MD 20742

A comprehensive analysis developed to evaluate plain trailing-edge flap systems for primary control is used to conduct a parametric study for a two-bladed teetering rotor of an ultralight helicopter. The analytical model includes a teetering rotor formulation, and a coupled trim procedure for determining trailing-edge flap inputs. A correlation study for the basic conventional rotor (primary pitch feather controls) was performed using calculations from another comprehensive analysis. The results show good agreement for blade natural frequencies, rotor collective and cyclic pitch controls, and shaft tilts. Calculations of required trailing-edge flap deflections, blade pitch angles, and actuation requirement are carried out at different advance ratios. With use of pitch indexing angle of 12° , the flap deflection and actuation requirement are small in the covered range of advance ratios. The parametric study shows that pitch index angle, flap location, flap length and chord ratio are critical parameters in determining flap deflection and actuation requirement.

Introduction

The basic swashplate control concept was invented in the 1930s, and the mechanism imposes the blade pitch control directly at the blade root. Overall, it is a successful design because of its relative simplicity and reliability, and is routinely implemented on almost all helicopters. However, the system inherently involves numerous exposed linkages, bearings, push rods and hinges, which are maintenance intensive, inspection critical, costly and act as a significant source of drag. The weight, drag, and cost, as well as the probability of failure of the mechanical components of swashplate control system, provide an impetus to search for alternative forms of main rotor pitch control. With the recent emergence of smart material actuators of high energy density (Ref. 1), it appears that active trailing-edge flaps driven by newly developed, blade-embedded, electromechanical actuators may provide a feasible design solution for blade pitch controls. Trailing-edge flap system provides pitch change indirectly via blade elastic twist due to pitching moment variation

with flap deflections. The trailing-edge flap deflections can be accomplished either using a swashplate (such as the case with Kaman's rotorcraft) or using directly actuators placed in the rotating frame (swashplateless rotor system). Furthermore, trailing-edge flaps have also received considerable interest among rotorcraft engineers for active control of vibration and noise (Refs. 2–7). The use of a trailing-edge flap rotor for primary control appears attractive in the context of an actively controlled rotor, where embedded flaps can perform multiple functions. Additionally, multiple on-blade flaps may increase the redundancy of the flight control system. A recently envisaged NASA Revolutionary Concepts (REVCON) program will examine the feasibility of "swashplateless" helicopter flight, and the present study will be part of this investigation.

Early studies by Lemnios and Wei *et al.* (Refs. 8, 9) presented modeling and correlation for Karman's SH-2 rotor, which utilizes the servo-flap type system as a primary control device. Straub and Charles (Ref. 10) examined the preliminary requirements of the swashplateless design for an Advanced Rotor and Control System (ARCS) concept. A recent study by Ormiston, using a simple rigid rotor model, explored the feasibility of a swashplateless rotor with plain trailing-edge flaps (Ref. 11). This study identified that the blade

* Graduate Research Assistant, Student Member AHS.

† Alfred Gessow Professor and Director, Fellow AHS.

Presented at Heli Japan 2002, Tochigi, Japan, Nov 11-13, 2002.
Copyright © 2002 by Jinwei Shen and Inderjit Chopra. All rights reserved.

fundamental torsional frequency need to be lowered to values in the neighborhood of 1.5 to 2.5/rev, and pitch index angle (pre-collective) need to be incorporated for the implementation of this concept. In a recent study, the authors developed a comprehensive analysis (Ref. 12) for a swashplateless rotor with trailing-edge flaps based on UMARC (University of Maryland Advanced Rotorcraft Code) (Ref. 13). The analysis was carried out on a five-bladed bearingless rotor system (MD 900) with a soft pitch link (control frequency of 2.1/rev) for the wind tunnel trim conditions. A swashplateless rotor with plain flaps was shown to be trimmed successfully with a trailing-edge flap control system in the complete range of advance ratios. Furthermore, the required flap angles were found to be moderate with a proper selection of blade pitch index angle. A multicyclic controller was implemented to minimize vibratory hub loads with the swashplateless rotor system. The plain flaps were shown to have the capability of performing both primary rotor control, and active vibration control functions. Additionally, the authors conducted a numerical parameter study (Ref. 14) for a swashplateless design based on a modern bearingless rotor. Blade pitch index angle, blade root spring stiffness, trailing-edge flap location and size (length and chord ratio) were found to be key parameters in the design of a swashplateless rotor with trailing-edge flaps. The aeroelastic stability characteristics were compared between the swashplateless rotor and conventional swashplate rotor. Overall, the swashplateless rotor was found to be more stable than the conventional rotor.

The objective of the present study is to examine the potential of utilizing the plain trailing-edge flap system for primary control with the teetering rotor of an ultralight helicopter, and conduct a parametric study of various key design variables involved in the integrated design.

Analytical Model

The baseline rotor used in the present study is from a 1000 pound ultralight helicopter (ASI 496). This helicopter has a cruise speed of 61 knots, corresponding to advance ratio of 0.16 at the nominal rotor speed. The ASI 496 rotor is a 2-bladed teetering rotor, with the characteristics given in Table 1. The blades are attached together, and hinged at the rotational axis, and have no independent flap and lead/lag offset hinges. The blades have a common flapping axis, however each blade has a separate pitch bearing which allows cyclic and collective pitch change capability. The teetering design has the advantage of being mechanically simple with a lower number of parts, and is easy to maintain. The teetering head lets various forces from the blades balance

Table 1: Baseline Rotor (ASI 496) and Flap Properties

<u>Rotor Data</u>	
Rotor Type	Teetering
Number of Blades	2
Rotor Diameter	23 ft.
Rotor Speed	525 RPM
Chord	6.7 inch
Linear Twist Angle	-8°
Lock Number	5.01
Solidity	0.0309
Ct/σ	0.075
Undersling	3.45 inch
<u>T.E. Flap Data</u>	
Flap Type	Plain Flap
Spanwise Length	25 inch (0.18R)
Chordwise Size	25 % (Blade Chord)
Flap Midspan Location	0.82R

themselves. Since the teetering rotor is inherently stiff-in-plane, it is not subject to ground resonance instability. ASI 496 rotor has a precone of three degree built into the rotor hub in order to reduce the stresses in the blades. An undersling design is also adopted in order to reduce Coriolis forces induced by teetering motion. The rotor system is torsionally soft with the fundamental torsional frequency of 2.2/rev. This torsionally soft design is also appropriate for implementation of trailing-edge flaps for primary controls.

The baseline rotor analysis is adopted from UMARC (Refs. 13, 15). The modeling of the trailing-edge flap rotor is discussed in Refs. 12 and 14. The present analysis incorporates finite element methodology in space and time. In the analysis of the teetering rotor, it is necessary to treat two blades simultaneously because two blades are rigidly connected to each other and attached to the mast through a common flapping hinge. The blade is modeled as an elastic beam undergoing flap bending, lag bending, elastic twist, and axial deformation. The rotor blades are discretized into a finite number of beam elements, each with 15 degrees of freedom. Fifteen elements are used to model the main blade. The trailing-edge flap is typically modeled using 4 elements. The coupled blade response and the trim control settings are solved simultaneously for the propulsive trim condition. Eight time elements with fifth order shape functions are used to calculate the coupled trim solution. The trailing-edge flap motion is prescribed, and as such dynamics of smart actuator is neglected for this study (Ref. 6). A quasi-steady model adapted from Theodorsen's theory (Ref. 16) is used to model the aerodynamic forces of the trailing-edge flap.

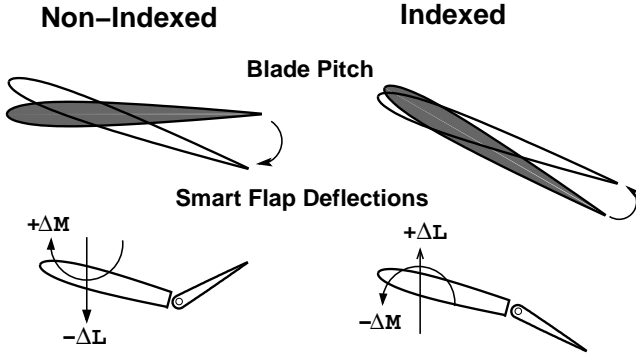


Figure 1: Blade pitch indexing

The Drees linear inflow is used to obtain the induced inflow distribution over the rotor disk.

Analysis of Trailing-edge Flap Rotor

For a rotor with trailing-edge flaps for primary control, the flaps produce torsional moment changes, which impel the main blades to free-fly against the root spring to achieve aerodynamic equilibrium, thereby producing the desired collective and cyclic blade twist. The trim variables for a flapped rotor are flap collective deflection, δ_0 , and flap cyclic deflections, δ_{1c} and δ_{1s} .

In order to reduce actuation forces, the rotor must be designed with torsionally soft blades, which can be achieved using soft root springs. To reduce the range of trailing-edge flap deflections, the rotor blades need to be pitched with a nose-up preset angle, which is normally higher than is required to trim the helicopter. As the rotor is accelerated to its rotational speed, the additional nose-down pitching moment generated by the flaps will twist the blade nose-down to the desired pitch position. The pre-collective pitch defines the blade root pitch angle at which the root spring results in a zero static load. This blade pitch index angle is an important design parameter that affects rotor performance and flap actuation requirements (Fig. 1). For a non-indexed blade, the flaps need to be deflected extremely large angles upward, in order to twist the blade nose-up to achieve desired angles of attack. However, for a pitch-indexed blade, the flaps are only required to have a small deflection to obtain a desired torsional moment.

For a rotor with flaps for primary controls, the control angle input to a flap is given by;

$$\delta(\psi) = \delta_0 + \delta_{1c}\cos(\psi) + \delta_{1s}\sin(\psi) \quad (1)$$

and the blade pitch angle consists of the blade index angle plus the pitch induced by flap control inputs. The induced angle consists of two parts, pitch due to root spring and elastic twist along the blade;

$$\theta(\psi) = \theta_{index} + \phi_{root}(\psi) + \phi_{twist}(r, \psi) \quad (2)$$

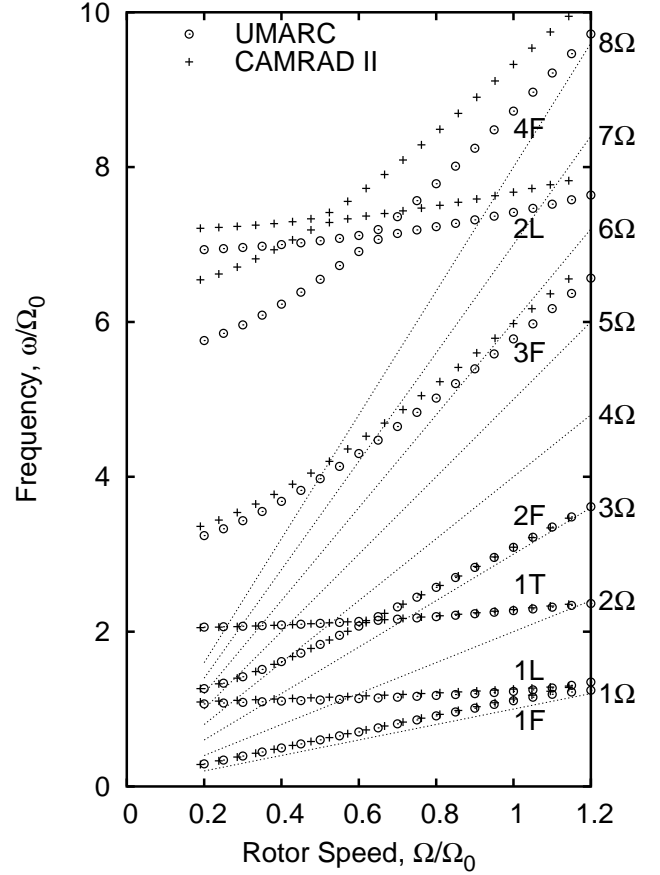


Figure 2: Comparison of blade normal mode frequency for ASI 496 teetering main rotor

The flap control angles are calculated from the coupled trim procedure. This procedure solves the vehicle trim equations and the blade steady response equations. For propulsive trim in a steady flight condition, the trim solution is obtained by solving the three force (vertical, longitudinal and lateral) and three moment (pitch, roll, yaw) vehicle equilibrium equations. For a specified gross weight and flight speed, the trim solution gives control angles, vehicle orientation (longitudinal and lateral shaft tilts) and tail rotor pitch. The control angles for conventional rotor are collective pitch (θ_0) and cyclic pitch (θ_{1c} , θ_{1s}) whilst for flapped rotor, they are collective flap (δ_0), and cyclic flap (δ_{1c} , δ_{1s}). The trim solution and blade responses are updated iteratively until the convergence criteria are satisfied. The incremental lift and pitching moment of an active trailing-edge flap, consisting of both inertial and aerodynamic contributions, are included in this coupled trim procedure.

Results and Discussion

Before the results of a rotor with trailing-edge flaps are investigated, the predictive capability of present comprehensive analysis is evaluated for a baseline teetering rotor (without trailing-edge flaps). Since there is no measured data available, the predictions of present analysis are compared with calculations from CAMRAD II (Refs. 17, 18). The calculated results of blade natural frequencies, trim angles, blade flapping angle, and main rotor power are correlated. Following this, the predicted results of the flapped rotor with the embedded flaps are presented, and the effects of various important design variables are investigated.

Baseline Correlation

The predictive capability of present analysis is evaluated by comparing the calculated results with predictions from CAMRAD II for the baseline ASI 496 rotor (without trailing-edge flap). The rotor characteristics are given in Table 1. The fuselage has a forward longitudinal CG offset from the rotor hub of 0.75 inch, and the vertical fuselage CG position is located below the hub of 50.6 inch. The main shaft has a built in forward tilt of 2 degrees.

Figure 2 compares computed natural blade frequencies from the present analysis with results obtained using CAMRAD II. Good agreement is seen for the first and second flatwise bending modes, the first chordwise mode, and the first torsion mode. Some discrepancy exists in the fourth flatwise bending mode and second inplane mode predictions. It may be due to differences in modeling assumptions since these higher order coupled modes are expected to be sensitive to them. Natural frequencies for the baseline rotor are summarized in Table 2 for the nominal rotating speed.

Figure 3 compares blade pitch, shaft tilt, flapping angles and main shaft power for the basic teetering rotor. Figure 3(a) shows the predicted values for blade collective pitch, longitudinal cyclic pitch and lateral cyclic pitch for different advance ratios. Good agreement is seen between two sets of results.

Figure 3(b) shows the prediction of rotor shaft angles for different advance ratios. Good agreement is seen for the longitudinal shaft angles except UMARC predictions show a slightly higher value at high advance ratio. Lateral shaft tilt angles are shown to have the same trend between the calculations of UMARC and CAMRAD II with a deviation of half degree. This may be due to the difference of inflow modeling used.

Figure 3(c) presents the calculation of blade flapping angle (or teetering angle) for various advance ratios. The longitudinal flapping angle is shown to agree well

Table 2: Calculated normal mode frequencies for ASI rotor at rotating speed of 525 RPM

Mode	Frequency (per rev)
1st flap	1.11
1st inplane	1.23
1st torsion	2.20
2nd flap	3.09
3rd flap	5.78
2nd inplane	7.42
4th flap	8.72

between the predictions of UMARC and CAMRAD II. The lateral blade flapping angle shows some discrepancies between the two predictions. Again, this may be attributed to the differences in inflow modeling.

Figure 3(d) illustrates the computation of main rotor power for different advance ratios. Good agreement is seen for high advance ratios. For low advance ratios, UMARC predictions are lower than CAMRAD II predictions. This discrepancy may be due to different empirical factors used in the computation of main rotor shaft power between the two analyses.

Baseline flapped Rotor

The selected baseline rotor configuration for the trailing-edge flap system is a modified version of the ASI 496 rotor, with pitch index angle set to 12° . The baseline trailing-edge flap characteristics are given in Table 1. Trailing-edge flap motion is positive for downward deflection, and hinge moment is positive when its direction is “nose-up” (and “tail-down”).

Figure 4 shows the conventional and flapped rotor control settings and actuation requirement versus advance ratio. Figure 4(a) presents the trailing-edge flap deflection required to trim the flapped rotor for different advance ratios. The required half peak-to-peak values of trailing-edge flap deflections are shown to be below 3° , whilst the mean values are smaller than 6° for the complete range of advance ratios. The trailing-edge flap collective angle, δ_0 , is deflected upward to increase twist of the blade nose-up to the desired position. The amount of deflection is determined by the collective pitch angle required to trim the helicopter at different advance ratios (Figure 4(b)). The baseline rotor airfoil presents a nose-down aerodynamic pitching moment, C_m in the order of 0.06. As a result, the blade will pitch nose-down under the effect of the aerodynamic pitching moment, and the trailing-edge flap is deflected upward to bring the pitch to desired position. The longitudinal cyclic, δ_{1s} , and lateral cyclic, δ_{1c} , are adjusted to provide relatively same cyclic pitch as the conventional rotor for different advance ratios.

Figure 4(b) compares the conventional rotor blade

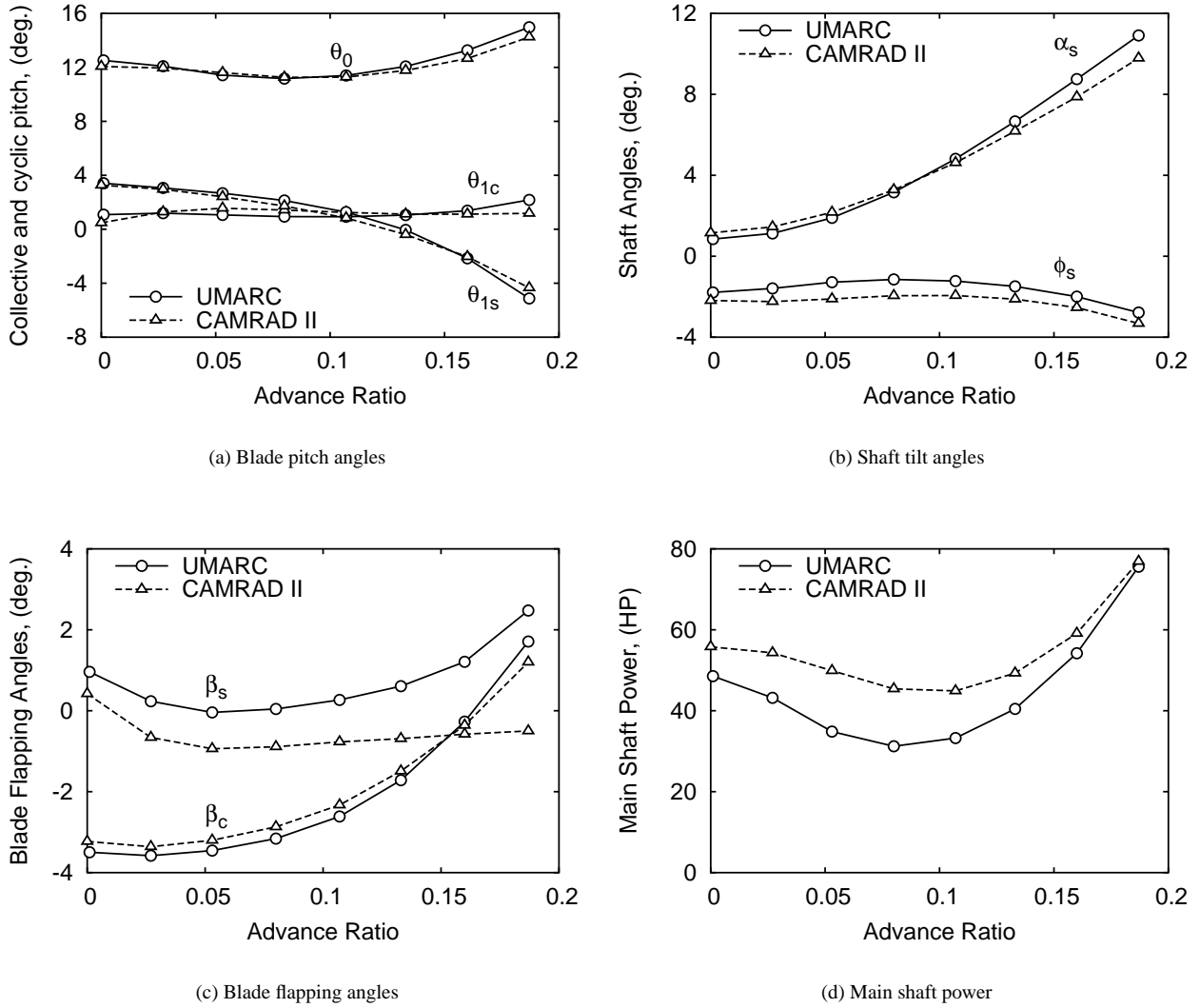


Figure 3: Comparison of blade pitch, shaft tilt, flapping angles, and main shaft power for the basic teetering rotor.

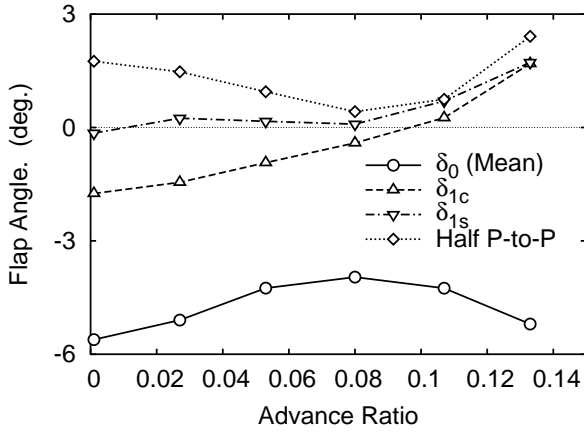
pitch angles with the equivalent flapped rotor blade pitch angles induced with the trailing-edge flaps. The blade pitch angles are displayed at the blade root. The blade longitudinal and lateral cyclic pitch of the flapped rotor exhibits similar trends to those of the conventional rotor, with a small difference attributable to the additional lift generated by the flap cyclic deflections, δ_{1s} and δ_{1c} .

Figure 4(c) illustrates flap actuation requirements at several advance ratios. The mean values of the hinge moments are generally determined by trailing-edge flap collective, δ_0 , and show same trend as the absolute value of collective flap angle versus advance ratio. The half peak-to-peak values of the hinge moments are determined by the flap cyclic deflection as well as the unsteadiness of the aerodynamic environment. The rapid increase of vibratory component of hinge moment at advance

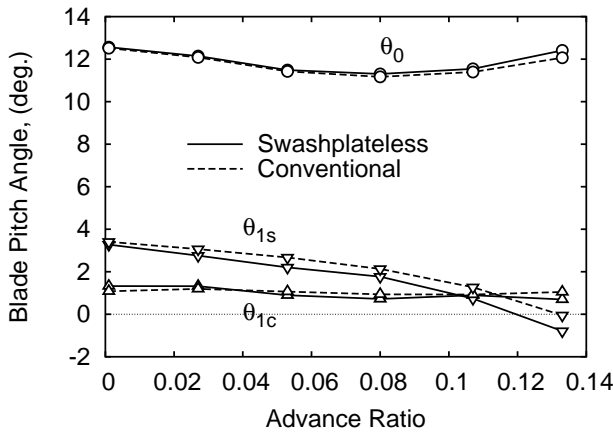
ratio of 0.13 is primarily due to an increment of the trailing-edge flap angle, and the aggravation of the unsteady aerodynamic environment. The actuation power is apparently dominated by the flap deflection amplitude and hinge moment. At an advance ratio of 0.08, the actuation power is a minimum due to the fact that the trailing-edge flap cyclic angles are small (as shown in Fig. 4(a)).

Blade Pitch Index Angle

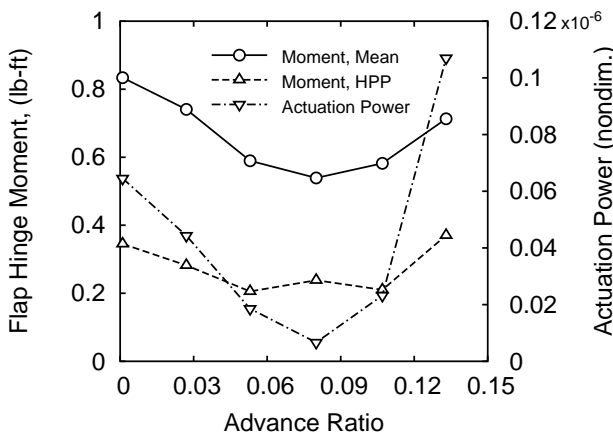
Figure 5 examines the effect of blade pitch index angle on the flap angle and actuation requirements. Figure 5(a) displays the flap deflections as a function of blade pitch index angle at an advance ratio of 0.08. As expected, the mean value of flap deflection, δ_0 , decreases with



(a) Trailing-edge flap angle



(b) Blade pitch



(c) Flap actuation requirement

Figure 4: Conventional and swashplateless rotor control settings and actuation requirement vs. advance ratio.

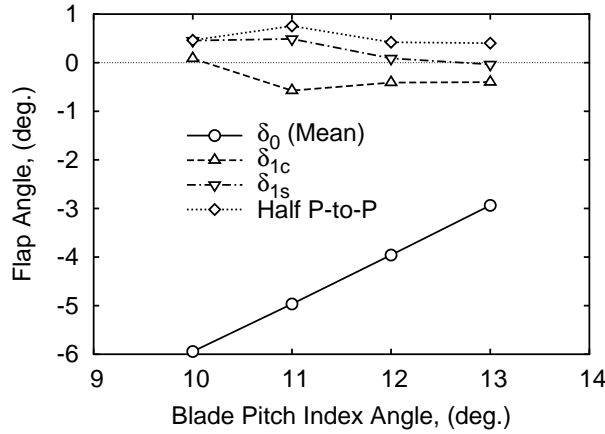
an increase of index angle. The half peak-to-peak value of flap deflection displays relatively small variation with index angle. This is due to the low cyclic pitch requirement at the advance ratio of 0.08. Figure 5(b) illustrates the actuation requirement variation with respect to the blade pitch index angle. The half peak-to-peak value of flap hinge moment shows a small change, and this is due to small variation of vibratory components of blade pitch angle and flap deflections. The mean value reduces rapidly due to the reduction of flap collective angle with increasing pitch index angle. The actuation power exhibits the minimum at the largest used index angle of 13° as a result of reduced hinge moment at this index angle. The initial increase of actuation power at index angle of 11° is due to a small increase of flap cyclic deflection. Figure 5 seems to suggest an optimal blade pitch index angle of 13° or may be even higher for an advance ratio of 0.08. The optimal pitch index angle varies with advance ratio due to the variation of required blade pitch. As a result, a compromise needs to be made in the selection of index angle to cover a complete range of flight speeds.

Trailing-edge Flap Spanwise Location

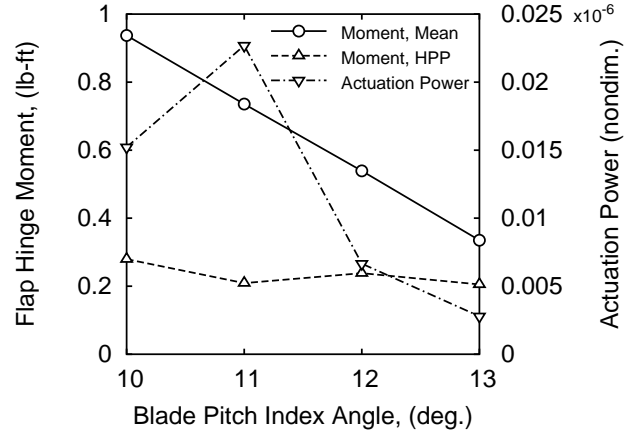
Flap spanwise location was identified as an important parameter in several studies utilizing flaps as active vibration control as well as primary control devices (Refs. 2, 3, 14). Figure 6(a) presents both the mean (collective) and cyclic components of flap deflections. A reduction in flap deflection, specially the mean value, takes place as the flap moves toward the blade tip. This is due to the fact that the flap effectiveness increases when the flap is located near the blade tip, where high dynamic pressure exists. Figure 6(b) shows the actuation requirement variation with flap spanwise location. The mean and vibratory components of hinge moment exhibit a very small variation with flap location. This is due to the fact that the required flap deflection reduces with the flap located towards tip, however, this is compensated by the increase of flap effectiveness due to the higher dynamic pressure. The actuation power initially increases with outboard flap location, and then reduces as the flap mover further than $76\%R$. For a given baseline flap length of $18\%R$, Figure 6 suggests that positioning the flap close to the tip raises the flap effectiveness and reduces the actuation requirement.

Trailing-edge Flap Length

Figure 8 illustrates the variation of flap deflection and actuation requirements for a flap length ranging from $14\%R$ to $28\%R$, with the flap middle section located at $82\%R$. As may be expected, flap deflections, both collective and cyclic, reduce with increasing flap length,



(a) Trailing-edge flap deflection



(b) Flap actuation requirement

Figure 5: Effect of pitch index angle, advance ratio of 0.08, flap length of $18\%R$, chord ratio of 0.25, located at $82\%R$.

as illustrated in Figure. 8(a). Figure 8(b) shows the effect of flap length on actuation requirement. The mean of hinge moment reduces with increasing flap length due to the reduction in flap collective deflection. The vibratory component of hinge moment displays small variation because of two counteracting effects; reduction of flap cyclic angles and increase of flap effectiveness with increasing flap length. Overall, actuation power decreases substantially with a variation of flap length from $12\%R$ to $28\%R$. Keeping in view both the flap effectiveness and actuation requirement, Figure 8 suggests an optimal flap length of $28\%R$ or may be a larger length.

Trailing-edge Flap Chord Ratio

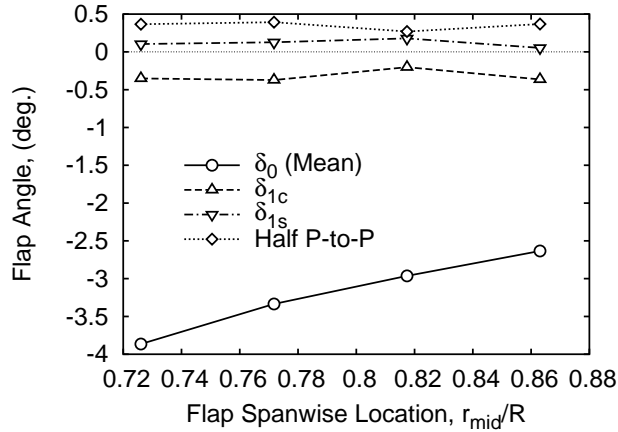
The flap chord ratio is a key design parameter because it plays an important role on flap lift and pitching moment. Previous test data and theoretical predictions related to fixed-wing trailing-edge flaps (Ref. 19) show that the flap pitching moment coefficient reaches a maximum around a flap chord ratio of 0.26, whilst the flap lift coefficients increase monotonically with flap chord ratio (Figure 7). Figure 9 presents the effect of trailing-edge flap chord ratio on flap deflection and actuation requirement. The flap chord ratio is varied from 0.15 to 0.45. Figure 9(a) shows both flap collective and cyclic deflections show a small variation with an increase in flap chord ratio from 0.15 to 0.25, and then increases at a faster rate afterward up to flap chord ratio of 0.45. This is due to the fact that the flap pitching moment coefficient reduces after flap chord ratio of 0.25. Figure 9(b) shows both the magnitude of mean and vibratory values of flap hinge moment increase largely with increasing flap chord ratio, which results from both the hinge moment coefficient increase

and the flap deflection increase. The actuation power increases with flap chord ratio, significantly more after a flap chord ratio of 0.25. Figure 9 suggests a small flap chord ratio of around 0.15 is optimum, when considering both flap effectiveness and actuation requirements.

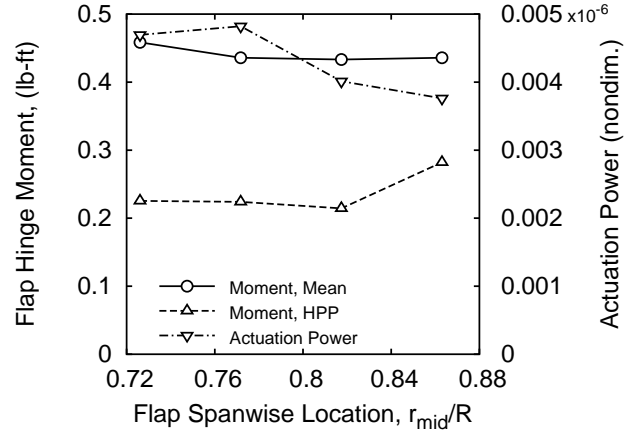
Conclusions

A comprehensive rotorcraft analysis for an ultralight helicopter with trailing-edge flaps for primary control was developed, and the actuation requirement for a range of forward speeds was evaluated. The baseline rotor is a teetering rotor, and the prediction capability of present analysis is correlated with the predictions of another comprehensive analysis (CAMRAD II). The correlation is carried out for the baseline rotor without trailing-edge flaps embedded. The predicted blade natural frequencies at different rotor rotating speeds were compared, and good agreement is generally seen except for two higher frequency modes (second inplane, fourth flap bending). The calculated rotor pitch angles, main shaft tilt angles and blade flapping angles are compared at different advance ratios between the two analyses. Rotor pitch, longitudinal shaft tilt, and longitudinal flapping angle compare well between two predictions whilst lateral shaft tilt and lateral flapping angles show some level of discrepancy, and this may be attribute to the differences in the inflow models used in the two analyses. Main shaft power compares well between the two analyses at high advance ratios whilst displays some difference at low advance ratios possibly due to different empirical factors used.

Calculations of required flap deflection, blade pitch



(a) Trailing-edge flap deflection



(b) Flap actuation requirement

Figure 6: Effect of flap spanwise location, advance ratio of 0.08, blade pitch index angle of 12° , flap length of $23\%R$, chord ratio of 0.25.

angles, and actuation requirement are carried out at different advance ratios. With use of pitch indexing angle of 12° , the flap deflection and actuation requirement are small in the covered range of advance ratios. Key design parameters, such as pitch index angle, flap location, flap length and chord ratio, were studied numerically. The major conclusions are summarized below:

1. An optimal selected pitch index angle reduces both the mean and cyclic components of required flap deflections, and as a result, minimizes the actuation power. The mean flap deflection reduces by 50% with increasing pitch index angle from 10° to 13° , and accordingly, the actuation power reduces approximately 80%.
2. Trailing-edge flaps located close to the blade tip where high dynamic pressure exists is found to be beneficial. The mean flap deflection is reduced approximately 30% by moving the flap from $72\%R$ to $87\%R$, and results in a 20% reduction in actuation power.
3. Large flap length is seen to be more effective in providing primary controls. It also reduces actuation power by lowering the required flap angles. The mean trailing-edge flap deflection reduces to almost one-half by doubling the size of the flap from $14\%R$ to $28\%R$, and actuation power is reduced approximately 90% accordingly.
4. Small flap chord ratio is more effective to provide aerodynamic pitching moment that is of key importance for primary controls with trailing-edge flaps. The study suggests a small flap chord ratio of

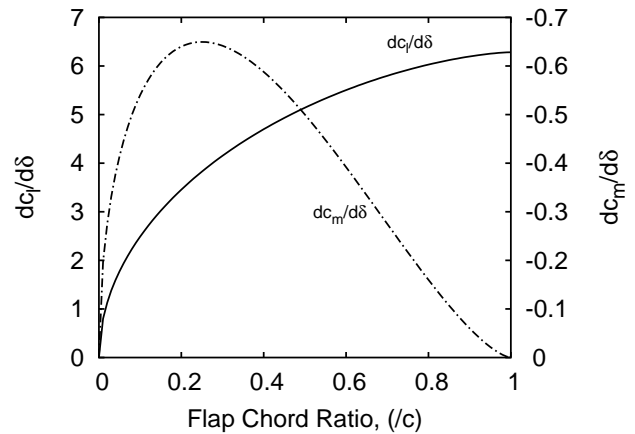
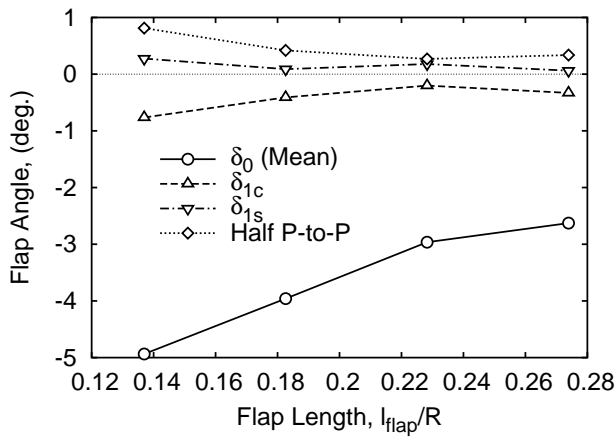


Figure 7: Theoretical lift and pitching moment characteristics of plain trailing-edge flaps

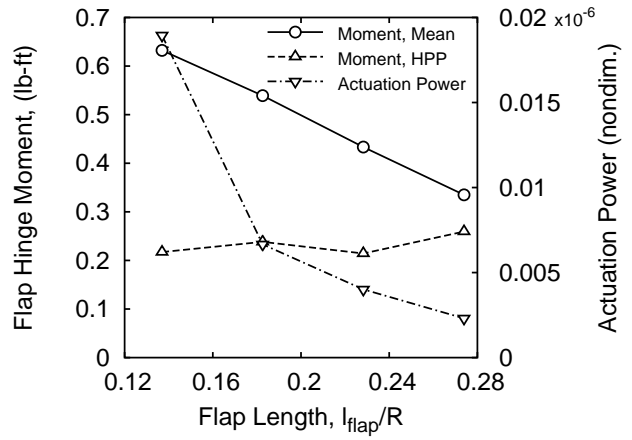
around 0.15 is beneficial for both flap effectiveness and actuation requirements.

Acknowledgments

The authors gratefully acknowledge Dr. Wayne Johnson (NASA/Ames) for providing the calculations of CAMRAD II as well as valuable advice and assistance. This work was supported by the NASA/Ames under grant NGT252273 with Dr. Chee Tung as technical monitor.

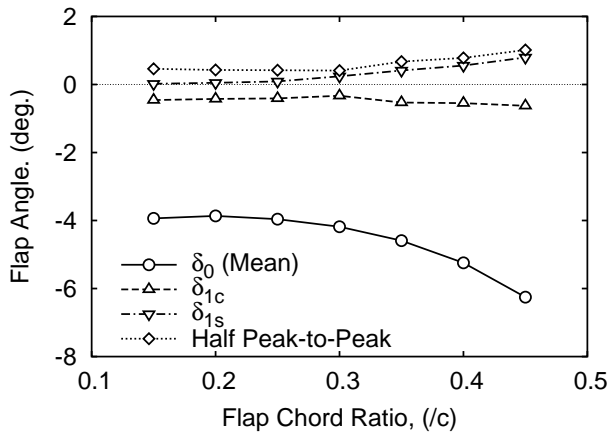


(a) Trailing-edge flap deflection

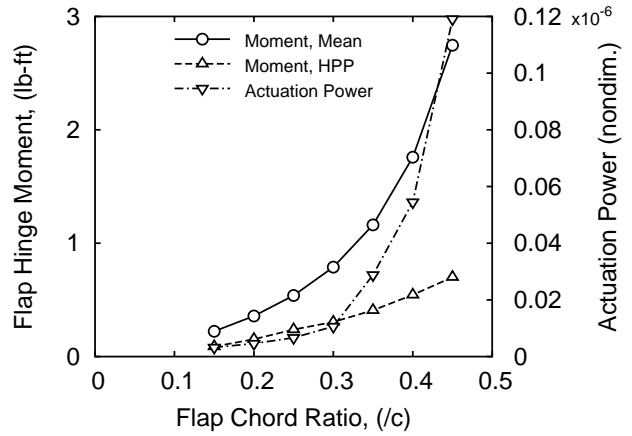


(b) Flap actuation requirement

Figure 8: Effect of flap length, advance ratio of 0.08, blade pitch index angle of 12° , flap chord ratio of 0.25, located at $82\%R$.



(a) Trailing-edge flap deflection



(b) Flap actuation requirement

Figure 9: Effect of flap chord ratio, advance ratio of 0.08, blade pitch index angle of 12° , flap length of $18\%R$, located at $82\%R$.

References

- ¹Chopra, I., "Status of Application of Smart Structures Technology to Rotorcraft Systems," *Journal of the American helicopter society*, Vol. 45, (4):228–252, October 2000.
- ²Millott, T. and Friedmann, P. "Vibration Reduction in Helicopter Rotors Using an Actively Controlled Partial Span Trailing Edge Flap Located on the Blades," Technical Report CR 4611, NASA, June 1994.
- ³Milgram, J., Chopra, I., and Straub, F., "Rotors with Trailing Edge Flaps: Analysis and Comparison with Experiment Data," *Journal of the American Helicopter Society*, Vol. 43, (4), October 1998.
- ⁴Koratkar, N. A. and Chopra, I. "Wind Tunnel Testing of a Mach-Scaled Rotor Model with Trailing-Edge Flaps,". In *Proceedings of the 56th Annual Forum of the American Helicopter Society*, Virginia Beach, May 2000.
- ⁵Shen, J. and Chopra, I. "Aeroelastic Modeling of Trailing-Edge Flaps with Smart Material Actuators,". In *Proceedings of the 41st AIAA/ASME/ASCE/AHS/ASC structure, structural dynamics, and materials conference*, AIAA-2000-1622, page 14, Atlanta, GA, April, 3-6 2000.
- ⁶Shen, J. and Chopra, I. "Aeroelastic Stability of Smart Trailing-Edge Flap Helicopter Rotors,". In *Proceedings of the 42nd AIAA/ASME/ASCE/AHS/ASC structure, structural dynamics, and materials conference*, AIAA-2001-1675, page 11, Seattle, WA, April, 16-19 2001.
- ⁷Straub, F. K. and Charles, B. D., "Aeroelastic Analysis of Rotors with Trailing Edge Flaps Using Comprehensive Codes," *Journal of the American Helicopter Society*, Vol. 46, :192–199, July 2001.
- ⁸Lemnios, A. Z. and Jones, R. "The Servo Flap – An Advanced Rotor Control System,". In *Proceedings of AHS and NASA Ames Research Center Vertical Lift Aircraft Design Conference*, San Francisco, CA, January, 17-19 1990.
- ⁹Wei, F.-S. and Jones, R., "Correlation and Analysis for SH-2F 101 Rotor," *Journal of Aircraft*, Vol. 25, (7):647–652, July 1988.
- ¹⁰Straub, F. and Charles, B. "Preliminary Assessment of Advanced Rotor/Control System Concepts (ARCS)," Technical Report 90-D03, USA AVSCOM, 1990.
- ¹¹Ormiston, R. A. "Aeroelastic Considerations for Rotorcraft Primary Control with On-Blade Elevons,". In *Proceedings of the 57th Annual Forum of the American Helicopter Society*, Washington, DC, May 2001.
- ¹²Shen, J. and Chopra, I. "Actuation Requirements for a Swashplateless Helicopter Control System With Trailing-Edge Flaps,". In *Proceeding of the 43rd AIAA/ASME/ASCE/AHS structures, structural dynamics, and materials conference and 10th AIAA/ASME/AHS adaptive structures conference*, number AIAA-2002-1444, page 11, Denver, Colorado, April 2002.
- ¹³Bir, G., Chopra, I., and et al. "University of Maryland Advanced Rotor Code (UMARC) Theory Manual," Technical Report UM-AERO 94-18, Center for Rotorcraft Education and Research, University of Maryland, College Park, July 1994.
- ¹⁴Shen, J. and Chopra, I. "A Parametric Design Study for a Swashplateless Helicopter Rotor with Trailing-Edge Flaps,". In *Proceedings of the AHS 58th Annual Forum*, page 15, Montreal, Canada, June 2002.
- ¹⁵Yeo, H. *A comprehensive vibration analysis of a coupled rotor/fuselage system*. PhD thesis, University of Maryland, College Park, MD, 1999.
- ¹⁶Theodorsen, T. and Garrick, I. E. "Nonstationary Flow about a Wing-Aileron-Tab Combination Including Aerodynamic Balance," Technical Report No. 736, NACA, 1942.
- ¹⁷Johnson, W. "Rotorcraft Aerodynamics Models for a Comprehensive Analysis,". In *Proceedings of the 54th Annual Forum of the American Helicopter Society*, Washington, DC, May 1998.
- ¹⁸Johnson, W. "Rotorcraft Dynamics Models for a Comprehensive Analysis,". In *Proceedings of the 54th Annual Forum of the American Helicopter Society*, Washington, DC, May 1998.
- ¹⁹Abbott, I. H. and Doenhoff, A. E. V. *Theory of wing sections*, chapter High-Lift Devices. Dover Publications, Inc., 1959.